Research Square

Preprints are preliminary reports that have not undergone peer review.
They should not be considered conclusive, used to inform clinical practice,
or referenced by the media as validated information.

Comprehensive Analysis of Lactylation-Related Genes in Peripheral T-Cell Lymphoma

Mengxue Ma
Fourth Hospital of Hebei Medical University
Lianjing Wang
Fourth Hospital of Hebei Medical University
Weijing Li
Fourth Hospital of Hebei Medical University
Wei Liu
Fourth Hospital of Hebei Medical University
Yun Feng
Fourth Hospital of Hebei Medical University
Yimin Zhang
Fourth Hospital of Hebei Medical University
Jiao Yan
Fourth Hospital of Hebei Medical University
Yunzhe Wang
Fourth Hospital of Hebei Medical University
Lihong Liu
46300554@hebmu.edu.cn

Fourth Hospital of Hebei Medical University

Research Article

Keywords:

Posted Date: September 11th, 2026

DOI: https://doi.org/10.21203/rs.3.rs-10848851/v1

License: This work is licensed under a Creative Commons Attribution 4.0 International License.
Read Full License

Additional Declarations: No competing interests reported.

Abstract

Background

Lactylation is an emerging post-translational modification that plays an important role in tumour progression. Peripheral T-cell lymphoma (PTCL) is a rare but highly heterogeneous subtype of non-Hodgkin lymphomas with limited effective therapeutic options. This study aimed to investigate the potential prognostic role of lactylation-related genes (LRGs) in PTCL.

Methods

Gene expression profiles and corresponding clinical data of patients with PTCL were obtained from the Gene Expression Omnibus database. LRGs were identified by integrating differentially expressed genes and genes positively correlated with the lactylation score. Key modules associated with the lactylation score were identified using weighted gene co-expression network analysis. Univariate Cox regression and random survival forest analyses were subsequently used to construct a prognostic model, which was further validated using the GSE90597 dataset. Functional enrichment, immune microenvironment, drug sensitivity, and model gene expression analyses were performed.

Results

Five key LRGs were identified and used to construct a lactylation-related prognostic model which was further evaluated in the GSE90597 dataset as exploratory external validation. The model effectively stratified patients with PTCL into high- and low-risk groups with distinct pathway enrichment, immune infiltration, and predicted drug sensitivity profiles. Notably, the high-risk group was significantly enriched in proliferation-related pathways and exhibited an immune-cold microenvironmental phenotype. In addition, the differential expression of the model genes between reactive lymph nodes and PTCL tumour tissues was validated using the GSE115917 and GSE263321 datasets.

Conclusion

The lactylation-related prognostic model may serve as a potential tool for prognostic assessment and individualised treatment stratification of PTCL, suggesting that lactylation-related molecular features may be involved in PTCL progression.

1. Introduction

Peripheral T-cell lymphoma (PTCL) is a rare and heterogeneous group of non-Hodgkin lymphomas (NHL) that arise from mature post-thymic T cells and accounts for approximately 10% of all NHLs [1]. PTCLs comprise a range of complex histological subtypes characterised by marked molecular heterogeneity,

diverse clinical manifestations, and aggressive behaviour [1,2]. The overall response to conventional anthracycline-based chemotherapy regimens, including CHOP, CHOEP, and dose-adjusted EPOCH, remains limited, with a 5-year overall survival (OS) rate of approximately 30% and poor long-term outcomes [1,2]. Therefore, there is an urgent need to further characterise the molecular and microenvironmental features of PTCL to improve risk stratification and develop more effective targeted therapeutic strategies, thereby ultimately improving patient survival.

The biological behaviour of PTCL is determined not only by the tumour cells themselves but also by cellular and non-cellular components within the tumour microenvironment [3,4]. Similar to other malignant cells, lymphoma cells exhibit the Warburg effect, whereby they preferentially take up glucose and generate lactate through glycolysis even under oxygen-rich conditions, resulting in substantial lactate accumulation within the lymphoma microenvironment [5,6]. In the lymphoma microenvironment, lactate is not merely a metabolic waste product; rather, it can contribute to immune evasion and lymphoma initiation and progression by modulating immune cell function, immune checkpoint expression, and key immunoregulatory pathways, such as mTOR signalling [5].

Lactylation is a recently discovered lactate-driven post-translational protein modification that mainly occurs on the lysine residues of histone and non-histone proteins. This epigenetic modification can remodel chromatin structure and subsequently regulate downstream gene transcription, thereby contributing to tumour progression [7,8]. The discovery of lactylation has expanded our understanding of the multifaceted roles of lactate in cancer. In diffuse large B-cell lymphoma, elevated lactate levels have been associated with higher serum lactate dehydrogenase (LDH) levels and higher maximum standardised uptake values, suggesting that lactylation may also serve as an important link between metabolic reprogramming, epigenetic regulation, and the lactate-rich microenvironment in lymphoma [9]. In contrast, little is known about the role of lactylation in PTCL, despite its highly aggressive clinical course and the fact that elevated LDH is an important clinical indicator of adverse prognosis.

To investigate the relationship between lactylation and PTCL and explore its potential biological implications, we analysed publicly available transcriptomic data to evaluate the potential of lactylation-related genes (LRGs) as prognostic biomarkers in PTCL and developed a lactylation-related prognostic model, with the aim of providing new insights into prognostic stratification and the development of molecularly targeted therapies for PTCL.

2. Methods

2.1 Data sources

PTCL-related gene expression datasets were retrieved from the Gene Expression Omnibus (GEO) database using the ‘GEOquery’ R package. The datasets used in this study included GSE58445, GSE90597, and GSE115917, whereas gene expression data from reactive lymph nodes were obtained from GSE263321 [10–14]. Based on previous studies, eight lactate metabolism- and phenotype-related

gene sets were selected from the Molecular Signatures Database (ESM 1), whereas a curated lactylation-associated gene set (n = 332) was compiled from published studies (ESM 2) [15–19].

2.2 Differential gene expression analysis

After the training cohort was stratified according to the optimal cutoff value of the lactylation score, differential gene expression between the high- and low-lactylation-score groups was analysed using the 'limma' R package. Differentially expressed genes (DEGs) were identified using the following criteria: $|log2FC| > 0.75$ and an adjusted $P < 0.05$.

2.3 Weighted gene co-expression network analysis (WGCNA)

The 'WGCNA' R package was used to construct a co-expression network associated with the lactylation score. After filtering the expression matrix of the training cohort according to non-coding/low-confidence genes, missingness, standard deviation, and median absolute deviation (MAD), the top 8,000 genes ranked by MAD were retained for analysis. Based on the scale-free topology fit index, the minimum soft-thresholding power satisfying $R^2 > 0.8$ was selected to construct the co-expression network, followed by the generation of the topological overlap matrix (TOM). Hierarchical clustering was subsequently performed based on 1-TOM, and co-expression modules were identified using a dynamic tree-cutting algorithm. The minimum module size was set to 30 genes and the module merging threshold was set to 0.25. Key modules were identified using Pearson's correlation analysis between module eigengenes and lactylation scores. The module showing the strongest correlation with the lactylation score was selected for subsequent analyses.

2.4 Functional enrichment analysis

Single-sample gene set enrichment analysis (ssGSEA), as implemented in the 'GSVA' R package, was used to calculate lactylation and lactate metabolism enrichment scores for each sample. Gene Ontology (GO) and Kyoto Encyclopedia of Genes and Genomes (KEGG) enrichment analyses were performed using the 'clusterProfiler' R package. In addition, gene set variation analysis (GSVA) was used to calculate Hallmark pathway activity scores for each sample, and differences in pathway activity between the high- and low-risk groups were compared using the 'limma' R package.

2.5 Immune infiltration analysis

ESTIMATE, ssGSEA, and microenvironment cell population-counter (MCP-counter) algorithms were applied to the gene expression profiles of the training cohort to characterise the tumour immune microenvironment and quantify immune infiltration status.

Immune infiltration scores and the expression levels of immune checkpoint-related genes were subsequently compared between the high- and low-risk groups, and their correlations with risk scores were evaluated using Spearman correlation analysis.

2.6 Drug response prediction

Drug-response area under the curve (AUC) data from the Cancer Therapeutics Response Portal version 2.0 and cell-line expression profiles from DepMap and the Cancer Cell Line Encyclopedia were used to develop a ridge regression model for predicting drug-response AUC values in patients from the training cohort. Differences in the predicted drug sensitivity between the high- and low-risk groups were compared.

2.7 Statistical analysis

All statistical analyses were performed using the R software (version 4.2.2). Kaplan–Meier survival curves were used to evaluate survival differences between patient groups, and comparisons were performed using the log-rank test. Cox proportional hazards regression models were used to assess the association between the risk score, clinical variables, and OS. Time-dependent receiver operating characteristic (ROC) curves and the corresponding AUCs were used to evaluate the predictive performance of the prognostic model at different time points. Continuous variables were compared between the two groups using the Wilcoxon rank-sum test, and correlations were evaluated using Spearman's correlation analysis. Multiple testing was performed using the Benjamini–Hochberg method. Statistical significance was set at $P < 0.05$.

3. Results

3.1 Prognostic value of lactylation in peripheral T-cell lymphoma

To investigate whether lactylation is involved in PTCL and assess its potential prognostic value, we used eight lactate metabolism- and phenotype-related gene sets and a curated LRG set. The ssGSEA algorithm was used to separately calculate lactate metabolism and lactylation scores for individual patients in the GSE58445 PTCL cohort. The patients were then divided into high- and low-score groups according to the optimal cutoff values. Kaplan–Meier survival analysis showed that patients with high lactate metabolism scores had significantly poorer OS (HR = 1.59, 95% CI: 1.03–2.45, log-rank P = 0.034; Fig. 1A). Similarly, patients with high lactylation scores showed poorer OS (HR = 1.74, 95% CI: 1.15–2.65, log-rank P = 0.009; Fig. 1B). In addition, the two scores were significantly positively correlated across the entire cohort (Spearman's $\rho = 0.392$, $P < 0.001$). These findings suggest a potential association between the activation of lactylation-related transcriptional programs and lactate metabolic reprogramming, indicating that these processes may be involved in PTCL progression and adverse prognosis.

3.2 Identification of lactylation-related genes in Peripheral T-cell lymphoma

To further identify key genes associated with lactylation in PTCL, differential gene expression analysis was performed between the high- and low-lactylation-score groups using thresholds of $|\log2FC| > 0.75$ and adjusted $P < 0.05$. Overall, 129 upregulated and 428 downregulated genes were identified (Fig. 2A).

Genes with a correlation coefficient > 0.3 and adjusted P < 0.05 were considered positively correlated with the lactylation score, resulting in the identification of 117 positively correlated DEGs.

Subsequently, a WGCNA network was constructed. A scale-free topology fit index > 0.8 was adopted, and the soft-thresholding power (β) was set to 12 (Fig. 2B). After filtering out low-expression genes, the top 8,000 highly variable genes were included in the network construction. Thirteen co-expression modules were identified. Among them, the pink module, containing 180 genes, showed the strongest positive correlation with the lactylation score (correlation = 0.44, P < 0.001; Fig. 2C–E), and was therefore identified as the key module. Intersecting the genes in this module with positively correlated DEGs yielded 47 LRGs for subsequent analysis (Fig. 2F).

3.3 Functional enrichment analysis of lactylation-related genes

GO and KEGG enrichment analyses were performed to further clarify the potential biological functions of LRGs in PTCL. GO analysis showed that in the biological process category, LRGs were mainly enriched in mitotic nuclear division, chromosome segregation, and spindle assembly. In the cellular component category, they were mainly associated with chromosomes, spindles, and microtubules. In the molecular function category, LRGs were predominantly associated with microtubule binding, catalytic activity on DNA, and ATP-dependent activity on DNA (Fig. 3A). KEGG analysis further showed that LRGs were primarily enriched in pathways such as the cell cycle, motor proteins, and homologous recombination (Fig. 3B). Collectively, these findings indicate that the 47 LRGs were predominantly associated with cell cycle progression, mitotic regulation, chromosome segregation, and DNA damage repair.

3.4 Construction of a lactylation-related prognostic model

Univariate Cox regression analysis was performed on the 47 LRGs, and 18 genes significantly associated with prognosis were identified (P < 0.05) (Fig. 4A). The random survival forest (RSF) algorithm was used to evaluate the importance of these genes (Fig. 4B), and the five top-ranked genes were selected to construct a multivariable Cox regression prognostic model. The risk score was calculated as follows: Risk score = (0.231 × KIF15) + (0.120 × MKI67) + (0.230 × RAD54L) − (0.090 × CDCA8) − (0.146 × FOXM1). Based on the optimal cutoff value, patients in the GSE58445 training cohort were classified into high- and low-risk groups. Kaplan–Meier analysis showed that patients in the high-risk group had significantly poorer survival than those in the low-risk group (HR = 2.30, 95% CI: 1.51–3.48, log-rank P < 0.001; Fig. 4C). Time-dependent ROC curve analysis was further used to assess the predictive performance of the lactylation-related prognostic model, yielding AUC values of 0.71, 0.62, and 0.63 at 1, 3, and 5 years, respectively (Fig. 4D).

Given the scarcity of publicly available PTCL datasets with survival information, an exploratory external validation was performed using the GSE90597 dataset, which included 55 patients with NK/T-cell lymphoma, a subtype of PTCL. Patients in the high-risk group had poorer survival outcomes. The 1- and 3-year AUC values were 0.63 and 0.68, respectively; the 5-year AUC could not be calculated because of

the limited follow-up duration in the validation cohort (Fig. 4E–F). These findings provide exploratory evidence that the model may have prognostic value in this PTCL subtype.

To assess the independent prognostic value of the prognostic model, univariate and multivariate Cox regression analyses were performed on both the GSE58445 and GSE90597 datasets. As shown in Table 1, patients in the high-risk group of the GSE58445 cohort had a significantly increased risk of death, and this association remained statistically significant after adjusting for clinical characteristics, such as age and sex. Consistent findings were observed in the external validation cohort, in which risk classification remained an independent prognostic factor for OS in multivariate Cox analysis. These findings suggest that this prognostic model provides stable, reliable, and independent prognostic information.

Table 1
Univariate and multivariable Cox regression analyses in the GSE58445 and GSE90597 datasets.

Variable	Univariate analysis			Multivariate analysis		
	HR	95% CI	P	HR	95% CI	P
Training group						
Risk (High/Low)	2.30	1.51–3.48	< 0.001	2.65	1.64–4.27	< 0.001
Sex (Male/Female)	1.59	0.98–2.59	0.0620	1.72	1.05–2.82	0.0300
Age (≥ 60/< 60 y)	1.37	0.86–2.19	0.1824	1.40	0.88–2.24	0.1587
Validation group						
Risk (High/Low)	2.60	1.25–5.39	0.0102	2.78	1.31–5.89	0.0075
Sex (Male/Female)	1.66	0.75–3.70	0.2138	1.93	0.85–4.41	0.1168
Age (≥ 60/< 60 y)	2.95	1.43–6.09	0.0033	2.74	1.32–5.70	0.0070

3.5 Functional characteristics of the high- and low-risk groups

GSVA showed that pathways related to the cell cycle, proliferation, and metabolic reprogramming, including E2F targets, G2/M checkpoints, MYC targets V1/V2, DNA repair, mTORC1 signalling, and oxidative phosphorylation, were significantly activated in the high-risk group. In contrast, inflammation- and immune-related pathways, including TNF-α signalling via NF-κB, inflammatory response, complement, and IL-6/JAK/STAT3 signalling, were broadly suppressed (Fig. 5A). In addition, correlation analysis between the lactylation-related risk score and classical oncogenic pathways in PTCL showed that the risk score was significantly positively correlated with MYC targets V1 and significantly negatively

correlated with TNF-α signalling via NF-κB and IL-6/JAK/STAT3 signalling (Fig. 5B). These findings indicate that the high-risk group is characterised by a highly proliferative tumour phenotype accompanied by the downregulation of inflammatory and immune-related signalling.

3.6 Immune infiltration analysis

To characterise the tumour immune microenvironment of the high-risk group, immune scores, immune checkpoint gene expression, and immune cell infiltration were systematically evaluated. The ImmuneScore, StromalScore, and ESTIMATEScore were significantly lower in the high-risk group than in the low-risk group, and all three scores were negatively correlated with the risk score (Fig. 6A–C), indicating an overall depletion of immune and stromal components in the high-risk group. The overall expression of immune checkpoint genes was lower in the high-risk group than in the low-risk group. Correlation analysis further showed that multiple immune checkpoint genes, including IDO1, NT5E, VSIR, CD274, CD276, PDCD1LG2, and ICOSLG, were significantly negatively correlated with the risk score (FDR < 0.05; Fig. 6D).

The ssGSEA-based immune cell infiltration analysis revealed an overall trend toward reduced immune infiltration in the high-risk group. Compared with the low-risk group, the infiltration scores for total macrophages, monocytes, M1 macrophages, dendritic cells, B cells, CD4 + T cells, neutrophils, and mast cells were significantly lower in the high-risk group (FDR < 0.05; Fig. 6E). Notably, Th2 cells were the only immune cell subset that showed significantly increased infiltration in the high-risk group. MCP-counter analysis further characterised the stromal and myeloid cell distributions within the microenvironment and demonstrated a significantly lower abundance of fibroblasts, endothelial cells, monocytes, and neutrophils in the high-risk group than in the low-risk group (Fig. 6F).

Collectively, these findings indicate that high-risk PTCL is characterised by an immune-cold microenvironment, with depletion of immune cells and stromal components, together with reduced immune checkpoint expression.

3.7 Prediction of therapeutic response

The predicted sensitivity of the patient cohort to multiple drugs was evaluated to explore the potential clinical benefits of chemotherapy and targeted therapy in high-risk patients. The high-risk group showed significantly greater predicted sensitivity to the bromodomain and extra-terminal (BET) inhibitors I-BET151 ($P = 2.18 \times 10^{-7}$) and JQ1 (P = 0.00678), and to the mitotic kinase inhibitor tozasertib (P = 0.00144) and the proteasome inhibitor bortezomib (P = 0.0223). In addition, increased sensitivity to the multi-kinase inhibitors lapatinib (P = 0.00678) and lenvatinib (P = 0.0492) was observed in the high-risk group (Fig. 7A-B). In contrast, no significant differences in the predicted sensitivity to conventional chemotherapeutic agents such as vincristine and paclitaxel were observed between the two groups. These findings suggest that high-risk patients may benefit from selected targeted therapeutic approaches and highlight the potential clinical value of treatment stratification based on a lactylation-related prognostic model.

3.8 Expression assessment of prognostic model genes

To investigate the expression patterns of the model genes, gene expression data from 14 PTCL samples and seven reactive lymph node samples in the GSE115917 and GSE263321 datasets, respectively, were analysed. As shown in Fig. 8, all five model genes were significantly upregulated in the tumour samples. These findings suggest that these genes may serve as candidate molecules for further investigation.

4. Discussion

PTCL is a group of aggressive and highly heterogeneous NHLs. The major pathological subtypes include peripheral T-cell lymphoma not otherwise specified (PTCL-NOS), T-follicular helper (TFH) lymphoma, and anaplastic large cell lymphoma [20]. Because PTCL is relatively rare and exhibits marked heterogeneity in its pathological origin and molecular genetic features, the identification of high-risk prognostic characteristics and the development of individualised therapeutic strategies remain major challenges in the management of PTCL.

Aberrant epigenetic regulation is a prominent mechanism underlying the development and progression of PTCL. The encouraging sensitivity of PTCL to epigenetic agents, including histone deacetylase and EZH1/2 inhibitors, has contributed to changes in the therapeutic landscape of PTCL [21,22]. However, the regulatory mechanisms underlying the epigenetic network in PTCL remain poorly understood, and the relationships between specific genetic alterations and responses to epigenetic therapies have not been fully clarified. DNA methylation and histone modification are among the most widely recognised epigenetic mechanisms involved [23,24]. Aberrant DNA hypermethylation promotes malignant phenotypes by silencing the transcription of tumour suppressor genes [23]. Previous studies have demonstrated recurrent mutations in DNA methylation-related regulators, including TET2, IDH2, and DNMT3A, in PTCL, particularly in angioimmunoblastic T-cell lymphoma and other PTCLs of TFH origin. In addition, DNMT3A was defined as a cytotoxic subgroup of PTCL-TBX21 that is associated with adverse outcomes [25,26].

Histone modification refers to specific post-translational modifications, such as acetylation and methylation, that remodel the chromatin structure and may subsequently result in the silencing of tumour suppressor genes or overexpression of oncogenes [24]. Studies have shown that a substantial proportion of PTCL-NOS cases harbour mutations in histone methylation-related genes, including KMT2D, SETD2, and KMT2A, as well as in histone acetylation-related genes such as EP300 and CREBBP. Mutations in histone modifier genes have also been identified as independent prognostic factors associated with shorter progression-free survival [27]. Moreover, abnormalities in histone modifications have been used as the basis for the molecular stratification of PTCL and are associated with distinct gene expression profiles and biological characteristics [3].

Lactylation is an emerging epigenetic regulation mechanism that plays an important role in tumour progression and immune microenvironment regulation in multiple cancers [7,8]. Although direct evidence of elevated lactate levels in PTCL tumour tissues remains limited, previous studies have shown that total lesion glycolysis was associated with an adverse prognosis in PTCL cohorts, suggesting the presence of metabolic reprogramming involving lactate production via the Warburg effect [28,29]. However, the role of lactylation in PTCL pathogenesis remains unclear. In the present study, we conducted an initial bioinformatics investigation of transcriptional features associated with the curated lactylation-related gene set in PTCL, providing new clues for understanding the pathogenesis of this disease.

We found that patients with PTCL who have high lactylation ssGSEA scores had poorer survival, consistent with previous findings that elevated lysine lactylation (Kla) levels are associated with adverse prognosis in T-cell lymphoma, suggesting the potential of lactylation-related features as prognostic biomarkers for PTCL [30]. Through a series of bioinformatic analyses, we identified 47 LRGs in PTCL and subsequently constructed a lactylation-related prognostic model for predicting OS.

The prognostic performance of the model was exploratorily evaluated in an independent NK/T-cell lymphoma cohort, a subtype of PTCL,in which patients in the high-risk group consistently exhibited significantly poorer survival than those in the low-risk group. ROC analysis supported the prognostic predictive performance of the model. Furthermore, after incorporating age and sex, multivariate regression analyses of both the training and validation cohorts supported the independent prognostic value of the model. Overall, our findings support an association between lactylation-related molecular features and PTCL prognosis. The lactylation-related prognostic model developed in this study consisted of KIF15, MKI67, RAD54L, CDCA8, and FOXM1, all of which are functionally associated with malignant tumour cell proliferation.

KIF15 is a member of the kinesin family that regulates cell division by participating in spindle assembly [31]. KIF15 is upregulated in multiple malignancies including lung, breast, and liver cancers, and its high expression is closely associated with adverse prognostic outcomes, suggesting its potential as a pan-cancer prognostic biomarker [32–34]. Furthermore, a previous study demonstrated that KIF15 recruits PGK1 and USP10 and enhances their interactions, thereby promoting glycolysis in pancreatic cancer cells. This finding suggests that KIF15 positively regulates lactate accumulation during tumour progression [35].

MKI67 encodes the Ki-67 protein, which is abundant during the active phases of the cell cycle but is rapidly degraded in the G0 phase, and is therefore widely used in clinical pathology as a marker of tumour proliferative activity [36]. Ki-67 is also used to assess tumour proliferation in PTCL and has been widely applied in risk stratification and prognostic prediction [37], suggesting that PTCL with a high lactylation score may be accompanied by increased proliferative activity. RAD54L encodes a DNA-dependent ATPase involved in DNA damage repair and homologous recombination [38]. A previous study demonstrated that under high intracellular lactate levels, MRE11 undergoes lactylation at K673, thereby enhancing DNA damage repair and promoting cisplatin resistance. This finding indicates that

lactylation may contribute to enhanced homologous recombination repair and is consistent with our functional enrichment results for the 47 LRGs [39].

CDCA8 encodes borealin, a component of the chromosome passenger complex that participates in key mitotic processes, including the maintenance of spindle stability and the promotion of chromosome segregation [40]. High CDCA8 expression has been reported as a marker of poor prognosis in multiple solid tumours. In lymphoma, CDCA8/Borealin expression has been reported to be at least 50% higher than that in normal tissues in approximately 30% of cases, although definitive evidence regarding specific lymphoma subtypes and prognostic associations remains limited [41,42]. FOXM1, a member of the FOXM subfamily, is an important transcription factor involved in cell-cycle regulation [43]. Previous studies have reported that FOXM1 positivity in PTCL is positively associated with disease stage and International Prognostic Index score, and negatively associated with OS [44], supporting FOXM1 as a potential mechanistic target in PTCL.

FOXM1 has also been linked to lactate metabolism in tumours. Studies of pancreatic cancer and hepatocellular carcinoma have shown that FOXM1 enhances glycolysis by activating glycolysis-related molecules, thereby promoting lactate production [45,46]. Additionally, a study of prostate cancer demonstrated that FOXM1 transcription is regulated by histone H3K18 lactylation, which promotes tumour proliferation and chemoresistance, suggesting that increased lactylation in a high-lactate environment may activate FOXM1 transcription [47]. Furthermore, compared with reactive lymph node tissues, KIF15, MKI67, RAD54L, CDCA8, and FOXM1 were significantly upregulated in PTCL tumour tissues, further supporting the biological plausibility of the prognostic model. Taken together, the known biological functions of these five genes were consistent with the functional enrichment profiles of the 47 LRGs, which were mainly associated with cell cycle progression, mitotic regulation, chromosome segregation, and DNA damage repair. These findings suggest a potential positive association between lactylation-related molecular features and PTCL progression and provide candidate lactylation-related targets for further mechanistic investigation.

GSVA showed enrichment of E2F targets, G2/M checkpoints, and MYC targets in the high-risk group, further supporting the idea that the prognostic model captures a highly proliferative subgroup of PTCL. In contrast, inflammatory and immune-related pathways, such as TNF-α/NF-κB signalling and the inflammatory response, were suppressed in the high-risk group, suggesting a potential association between lactylation-related features and immune escape in PTCL. Multiple studies have demonstrated that lactylation contributes to the remodelling of the tumour immune microenvironment by reprogramming tumour cells and tumour-infiltrating immune populations, including myeloid cells and macrophages [48,49].

Therefore, we further investigated the differences in the tumour microenvironment between the high- and low-risk groups. The high-risk group exhibited lower immune scores, lower immune checkpoint expression levels, and reduced immune cell infiltration. Collectively, these findings indicated an immune-depleted, immune-cold tumour phenotype. Similar associations between high lactylation levels and

immune-cold tumours have been observed in certain solid tumours. In addition, a study of hepatocellular carcinoma showed that the inhibition of YAP1-associated histone lactylation could promote the conversion of the tumour microenvironment toward an immune-hot state [48–50]. Previous studies have classified PTCL into stromal, TFH-like, inflammatory, and depleted microenvironmental subtypes. The depleted subtype exhibited features similar to those observed in the high-risk group in our study, including the depletion of immune and stromal components and the enrichment of proliferative features. An independent study further demonstrated that this depleted subtype is associated with poorer clinical outcomes, which is consistent with our findings [3,51].

Notably, despite the overall reduction in microenvironmental components, the high-risk group exhibited enhanced Th2-related transcriptional features. Previous work has shown that the depleted subtype is associated with 'Th2-ILs and GATA3 activation', suggesting that the Th2-related signal observed in our study may originate from the malignant cells themselves rather than from increased numbers of infiltrating immune cells [51].

We further explored potential therapeutic options for high-risk patients. The results showed that high-risk patients had a greater predicted sensitivity to selected drugs, including the BET inhibitors I-BET151 and JQ1, the mitotic kinase inhibitor tozasertib, the proteasome inhibitor bortezomib, and the multikinase inhibitors lapatinib and lenvatinib.

These findings support further investigation of individualised treatment stratification for patients with PTCL. However, validation using real-world clinical treatment response data is required.

Overall, this study systematically evaluated the potential value of lactylation-related features in PTCL and established a predictive model that may aid in the prognostic stratification of patients with PTCL. In particular, the model identified patient subgroups with distinct immune characteristics and predicted drug sensitivity. Nevertheless, further independent multicentre prospective cohort studies are required to determine whether this prognostic model can be incorporated into clinical practice. Owing to the lack of detailed clinical information in publicly available datasets, we were unable to investigate whether the integration of existing conventional prognostic models, such as the Prognostic Index for T-cell lymphoma (PIT) and modified PIT (mPIT), with lactylation-related transcriptomic features could improve the prognostic assessment of PTCL. Therefore, we plan to explore this issue in a patient cohort at our centre to facilitate more refined individualised treatment strategies.

This study has some limitations. First, all datasets used in the present study were obtained from public databases and analysed retrospectively, which may have introduced selection bias and cohort heterogeneity in terms of ethnicity, treatment strategies, and pathological subtypes. Moreover, although drug sensitivity in different patient subgroups was predicted computationally, direct treatment response data were not available to evaluate the actual clinical benefits of stratified therapies. Therefore, multicentre prospective clinical studies are required to further assess the robustness of the prognostic model. In addition, because of the limitations of publicly available datasets, detailed clinical

characteristics, treatment regimens, and pathological subtypes were not available for all cohorts, preventing the assessment of model applicability across different patient subgroups.

Second, although we selected a predefined lactylation-associated reference gene set, this gene set may not fully capture the complexity of the lactylation regulatory network and may therefore be subject to gene selection bias and omission.

Third, the present study was primarily based on bioinformatics analyses of transcriptomic data derived from bulk tumour tissues. Consequently, the observed transcriptional features could not be definitively assigned to malignant cells or components of the tumour microenvironment, particularly in immune microenvironment analyses. In addition, protein-level evidence is lacking and further investigations at the single-cell and proteomic levels are warranted. Finally, the absence of in vitro and in vivo functional experiments limits the mechanistic interpretation of how lactylation occurs in PTCL and how it influences tumour biological behaviour.

5. Conclusion

Despite these limitations, our study highlights the potential importance of lactylation-related molecular features in PTCL progression and prognosis and establishes a lactylation-related prognostic model that provides new insights into the identification of patients with different prognoses and potential for treatment stratification. Our analyses of predicted drug sensitivity and immune regulation in relation to the prognostic model further support lactylation-related biology as a promising area for investigation. Future studies exploring therapeutic strategies that target lactylation may provide new opportunities to improve the long-term survival of patients with PTCL.

Declarations

Funding statement

This study received no external funding.

Ethics statement

This study is a bioinformatics analysis based on publicly available databases. All data were obtained from public repositories and no human or animal subjects were involved. Therefore, ethical approval and informed consent were not required.

Author contributions

Mengxue Ma: Conceptualization, Methodology, Formal analysis, Writing – original draft.

Lianjing Wang, Weijing Li, Wei Liu, Yun Feng, Yimin Zhang, Jiao Yan, and Yunzhe Wang: Data curation, Validation, Writing – review & editing.

Lihong Liu: Conceptualization, Supervision, Writing – review & editing.

All authors read and approved the final manuscript.

Competing interest

The authors declare that they have no competing interests.

Dual publication

This manuscript has not been published elsewhere and is not under consideration by another journal. All authors have approved the manuscript and agree with its submission.

Data availability statement

The data analysed in this study are available in public repositories.

References

1. Shea L, Mehta-Shah N. Peripheral T-cell lymphoma: are all patients high risk? Blood. 2024;144(25):2604–2612. doi:10.1182/blood.2023020912.
2. Fiore D, Cappelli LV, Broccoli A, et al. Peripheral T cell lymphomas: from the bench to the clinic. Nat Rev Cancer. 2020;20(6):323–342. doi:10.1038/s41568-020-0247-0.
3. Huang YH, Qiu YR, Zhang QL, et al. Genomic and transcriptomic profiling of peripheral T cell lymphoma reveals distinct molecular and microenvironment subtypes. Cell Rep Med. 2024;5(2):101416. doi:10.1016/j.xcrm.2024.101416.
4. Sugio T, Miyawaki K, Kato K, et al. Microenvironmental immune cell signatures dictate clinical outcomes for PTCL-NOS. Blood Adv. 2018;2(17):2242–2252. doi:10.1182/bloodadvances.2018018754.
5. Zhou Y, Lou J, Tian Y, et al. How lactate affects immune strategies in lymphoma. Front Mol Biosci. 2024;11:1480884. doi:10.3389/fmolb.2024.1480884.
6. Yi HK, Yoo J, Kim SJ, et al. Lymphoma total lesion glycolysis leads to hyperlactatemia and reduction of brain glucose utilization. Sci Rep. 2022;12(1):12639. doi:10.1038/s41598-022-16562-z.
7. Zhang D, Tang Z, Huang H, et al. Metabolic regulation of gene expression by histone lactylation. Nature. 2019;574(7779):575–580. doi:10.1038/s41586-019-1678-1.
8. He Y, Song T, Ning J, et al. Lactylation in cancer: mechanisms in tumour biology and therapeutic potentials. Clin Transl Med. 2024;14(11):e70070. doi:10.1002/ctm2.70070.
9. Zhu M, Xiao Q, Cai X, et al. Predicting lymphoma prognosis using machine learning-based genes associated with lactylation. Transl Oncol. 2024;49:102102. doi:10.1016/j.tranon.2024.102102.
10. Davis S, Meltzer PS. GEOquery: a bridge between the Gene Expression Omnibus and BioConductor. Bioinformatics. 2007;23(14):1846–1847. doi:10.1093/bioinformatics/btm254.

11. Iqbal J, Wright G, Wang C, et al. Gene expression signatures delineate biological and prognostic subgroups in peripheral T-cell lymphoma. Blood. 2014;123(19):2915–2923. doi:10.1182/blood-2013-11-536359.
12. Ng SB, Chung TH, Kato S, et al. Epstein–Barr virus-associated primary nodal T/NK-cell lymphoma shows a distinct molecular signature and copy number changes. Haematologica. 2018;103(2):278–287. doi:10.3324/haematol.2017.180430.
13. Ganapathi KA, Nicolae A, Egan C, et al. Peripheral T-cell lymphomas expressing CD30 and CD15 expand the spectrum of anaplastic large cell lymphoma, ALK-negative. Br J Haematol. 2024;204(5):1862–1871. doi:10.1111/bjh.19442.
14. Miller I, Mumau MD, Shyamsundar S, et al. No evidence for active viral infection in unicentric and idiopathic multicentric Castleman disease by Viral-Track analysis. Sci Rep. 2025;15:1676. doi:10.1038/s41598-025-85193-x.
15. Liberzon A, Subramanian A, Pinchback R, Thorvaldsdóttir H, Tamayo P, Mesirov JP. Molecular Signatures Database (MSigDB) 3.0. Bioinformatics. 2011;27(12):1739–1740. doi:10.1093/bioinformatics/btr260.
16. Qiu S, Wang Y, Rao H, Que Q, Wu Y, Zhu R, et al. Tumor microenvironment-associated lactate metabolism regulates the prognosis and precise checkpoint immunotherapy outcomes of patients with lung adenocarcinoma. Eur J Med Res. 2022;27(1):256. doi:10.1186/s40001-022-00895-6.
17. Huang T, Lian D, Chen M, Liu Y, Zhang M, Zeng D, Zhou SK, Ying W. Prognostic value of a lactate metabolism gene signature in lung adenocarcinoma and its associations with immune checkpoint blockade therapy response. Medicine (Baltimore). 2024;103(40):e39371. doi:10.1097/MD.0000000000039371.
18. Cheng Z, Huang H, Li M, Liang X, Tan Y, Chen Y. Lactylation-related gene signature effectively predicts prognosis and treatment responsiveness in hepatocellular carcinoma. Pharmaceuticals (Basel). 2023;16(5):644. doi:10.3390/ph16050644.
19. Wan N, Wang N, Yu S, et al. Cyclic immonium ion of lactyllysine reveals widespread lactylation in the human proteome. Nat Methods. 2022;19(7):854–864. doi:10.1038/s41592-022-01523-1.
20. Alaggio R, Amador C, Anagnostopoulos I, et al. The 5th edition of the World Health Organization Classification of Haematolymphoid Tumours: lymphoid neoplasms. Leukemia. 2022;36(7):1720–1748. doi:10.1038/s41375-022-01620-2.
21. Shi Y, Dong M, Hong X, et al. Results from a multicenter, open-label, pivotal phase II study of chidamide in relapsed or refractory peripheral T-cell lymphoma. Ann Oncol. 2015;26(8):1766–1771. doi:10.1093/annonc/mdv237.
22. Zinzani PL, Izutsu K, Mehta-Shah N, et al. Valemetostat for patients with relapsed or refractory peripheral T-cell lymphoma (VALENTINE-PTCL01): a multicentre, open-label, single-arm, phase 2 study. Lancet Oncol. 2024;25(12):1602–1613. doi:10.1016/S1470-2045(24)00503-5.
23. Jones PA, Baylin SB. The epigenomics of cancer. Cell. 2007;128(4):683–692. doi:10.1016/j.cell.2007.01.029.

24. Kouzarides T. Chromatin modifications and their function. Cell. 2007;128(4):693–705. doi:10.1016/j.cell.2007.02.005.
25. Palomero T, Couronné L, Khiabanian H, et al. Recurrent mutations in epigenetic regulators, RHOA and FYN kinase in peripheral T cell lymphomas. Nat Genet. 2014;46(2):166–170. doi:10.1038/ng.2873.
26. Herek TA, Bouska A, Lone W, et al. DNMT3A mutations define a unique biological and prognostic subgroup associated with cytotoxic T cells in PTCL-NOS. Blood. 2022;140(11):1278–1290. doi:10.1182/blood.2021015019.
27. Ji MM, Huang YH, Huang JY, et al. Histone modifier gene mutations in peripheral T-cell lymphoma not otherwise specified. Haematologica. 2018;103(4):679–687. doi:10.3324/haematol.2017.182444.
28. Kitadate A, Narita K, Fukumoto K, et al. Baseline total lesion glycolysis combined with interim positron emission tomography-computed tomography is a robust predictor of outcome in patients with peripheral T-cell lymphoma. Cancer Med. 2020;9(15):5509–5518. doi:10.1002/cam4.3226.
29. Zhou Y, Zhang X, Qin H, et al. Prognostic values of baseline 18F-FDG PET/CT in patients with peripheral T-cell lymphoma. Biomed Res Int. 2020;2020:9746716. doi:10.1155/2020/9746716.
30. Yu Z, Zhou X, Cai Y, et al. Lactate-mediated histone H3K9 lactylation facilitates tumorigenesis of T-cell lymphoma via activation of SFXN1 expression. Blood. 2023;142(Suppl 1):1652. doi:10.1182/blood-2023-184663.
31. Tanenbaum ME, Macůrek L, Janssen A, et al. Kif15 cooperates with Eg5 to promote bipolar spindle assembly. Curr Biol. 2009;19(20):1703–1711. doi:10.1016/j.cub.2009.08.027.
32. Qiao Y, Chen J, Ma C, et al. Increased KIF15 expression predicts a poor prognosis in patients with lung adenocarcinoma. Cell Physiol Biochem. 2018;51(1):1–10. doi:10.1159/000495155.
33. Gao X, Zhu L, Lu X, et al. KIF15 contributes to cell proliferation and migration in breast cancer. Hum Cell. 2020;33(4):1218–1228. doi:10.1007/s13577-020-00392-0.
34. Li Q, Qiu J, Yang H, et al. Kinesin family member 15 promotes cancer stem cell phenotype and malignancy via reactive oxygen species imbalance in hepatocellular carcinoma. Cancer Lett. 2020;482:112–125. doi:10.1016/j.canlet.2019.11.008.
35. Quan G, Xu J, Wang J, et al. KIF15 is essential for USP10-mediated PGK1 deubiquitination during the glycolysis of pancreatic cancer. Cell Death Dis. 2023;14(2):137. doi:10.1038/s41419-023-05679-2.
36. Scholzen T, Gerdes J. The Ki-67 protein: from the known and the unknown. J Cell Physiol. 2000;182(3):311–322. doi:10.1002/(SICI)1097-4652(200003)182:3<311::AID-JCP1>3.0.CO;2-9.
37. Went P, Agostinelli C, Gallamini A, et al. Marker expression in peripheral T-cell lymphoma: a proposed clinical-pathologic prognostic score. J Clin Oncol. 2006;24(16):2472–2479. doi:10.1200/JCO.2005.03.6327.
38. Ceballos SJ, Heyer WD. Functions of the Snf2/Swi2 family Rad54 motor protein in homologous recombination. Biochim Biophys Acta. 2011;1809(9):509–523. doi:10.1016/j.bbagrm.2011.06.006.

39. Chen Y, Wu J, Zhai L, et al. Metabolic regulation of homologous recombination repair by MRE11 lactylation. Cell. 2024;187(2):294–311.e21. doi:10.1016/j.cell.2023.11.022.
40. Gassmann R, Carvalho A, Henzing AJ, et al. Borealin: a novel chromosomal passenger required for stability of the bipolar mitotic spindle. J Cell Biol. 2004;166(2):179–191. doi:10.1083/jcb.200404001.
41. Hu H, Umair M, Khan SA, et al. CDCA8, a mitosis-related gene, as a prospective pan-cancer biomarker: implications for survival prognosis and oncogenic immunology. Am J Transl Res. 2024;16(2):432–445. doi:10.62347/WSEF7878.
42. Date DA, Jacob CJ, Bekier ME, et al. Borealin is repressed in response to p53/Rb signaling. Cell Biol Int. 2007;31(12):1470–1481. doi:10.1016/j.cellbi.2007.06.013.
43. Wierstra I, Alves J. FOXM1, a typical proliferation-associated transcription factor. Biol Chem. 2007;388(12):1257–1274. doi:10.1515/BC.2007.159.
44. Feng HN, Shao XX, Bu P, et al. Expression of CDK6 and FOXM1 in peripheral T-cell lymphoma and their significance. Zhonghua Bing Li Xue Za Zhi. 2020;49(6):594–600. doi:10.3760/cma.j.cn112151-20191104-00710.
45. Cui J, Shi M, Xie D, et al. FOXM1 promotes the Warburg effect and pancreatic cancer progression via transactivation of LDHA expression. Clin Cancer Res. 2014;20(10):2595–2606. doi:10.1158/1078-0432.CCR-13-2407.
46. Shang R, Pu M, Li Y, et al. FOXM1 regulates glycolysis in hepatocellular carcinoma by transactivating glucose transporter 1 expression. Oncol Rep. 2017;37(4):2261–2269. doi:10.3892/or.2017.5472.
47. Sheng W, Li Y, Tan T, et al. Icariin-curcumol inhibits histone H3K18 lactylation and FOXM1 expression to enhance the sensitivity of prostate cancer cells to docetaxel. Cancer Cell Int. 2025;25:423. doi:10.1186/s12935-025-03927-3.
48. De Leo A, Ugolini A, Yu X, et al. Glucose-driven histone lactylation promotes the immunosuppressive activity of monocyte-derived macrophages in glioblastoma. Immunity. 2024;57(5):1105–1123.e8. doi:10.1016/j.immuni.2024.04.006.
49. Ma Z, Yang J, Jia W, et al. Histone lactylation-driven B7-H3 expression promotes tumor immune evasion. Theranostics. 2025;15(6):2338–2359. doi:10.7150/thno.105947.
50. Gao Y, Gong Y, Song X, et al. Dihydroartemisinin inhibits histone lactylation through YAP1 to act as a “hot” switch for “cold” tumor in hepatocellular carcinoma. Phytomedicine. 2025;148:157307. doi:10.1016/j.phymed.2025.157307.
51. Fiore D, Cappelli LV, Zhaoqi L, et al. A patient-derived T cell lymphoma biorepository uncovers pathogenetic mechanisms and host-related therapeutic vulnerabilities. Cell Rep Med. 2025;6(4):102029. doi:10.1016/j.xcrm.2025.102029

Figures

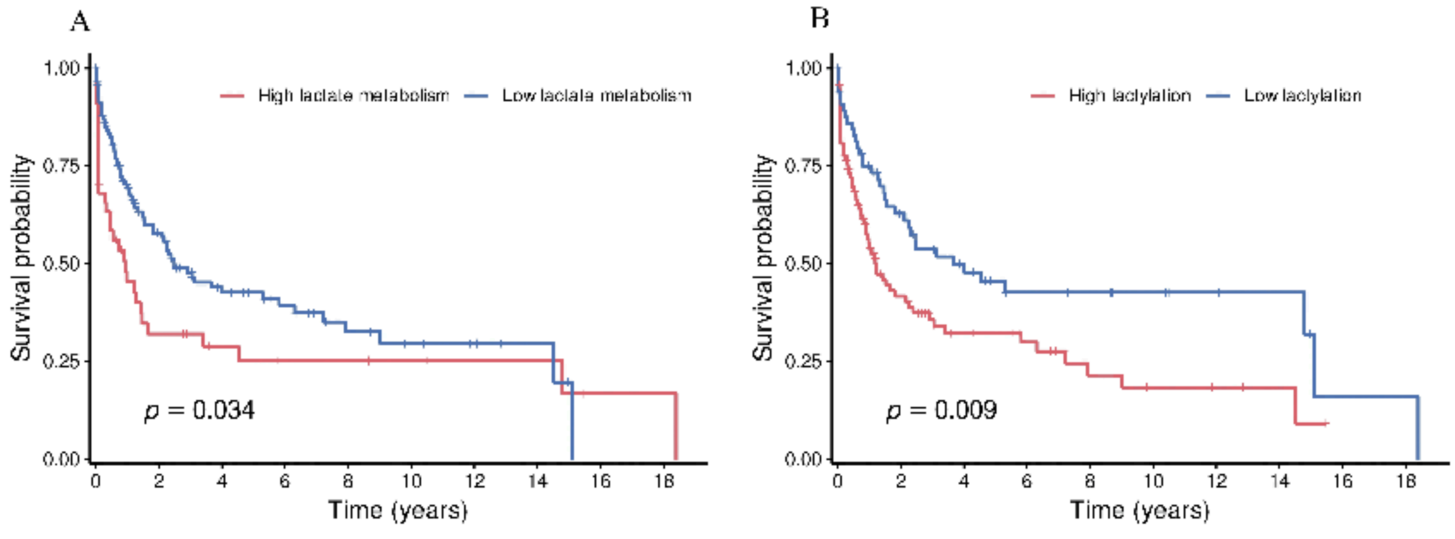


Figure 1

Association of lactate metabolism and lactylation scores with prognosis in patients with PTCL

(A) Kaplan–Meier survival analysis showing that patients in the high lactate metabolism score group had poorer overall survival (OS).

(B) Kaplan–Meier survival analysis showing that patients in the high lactylation score group had poorer OS.

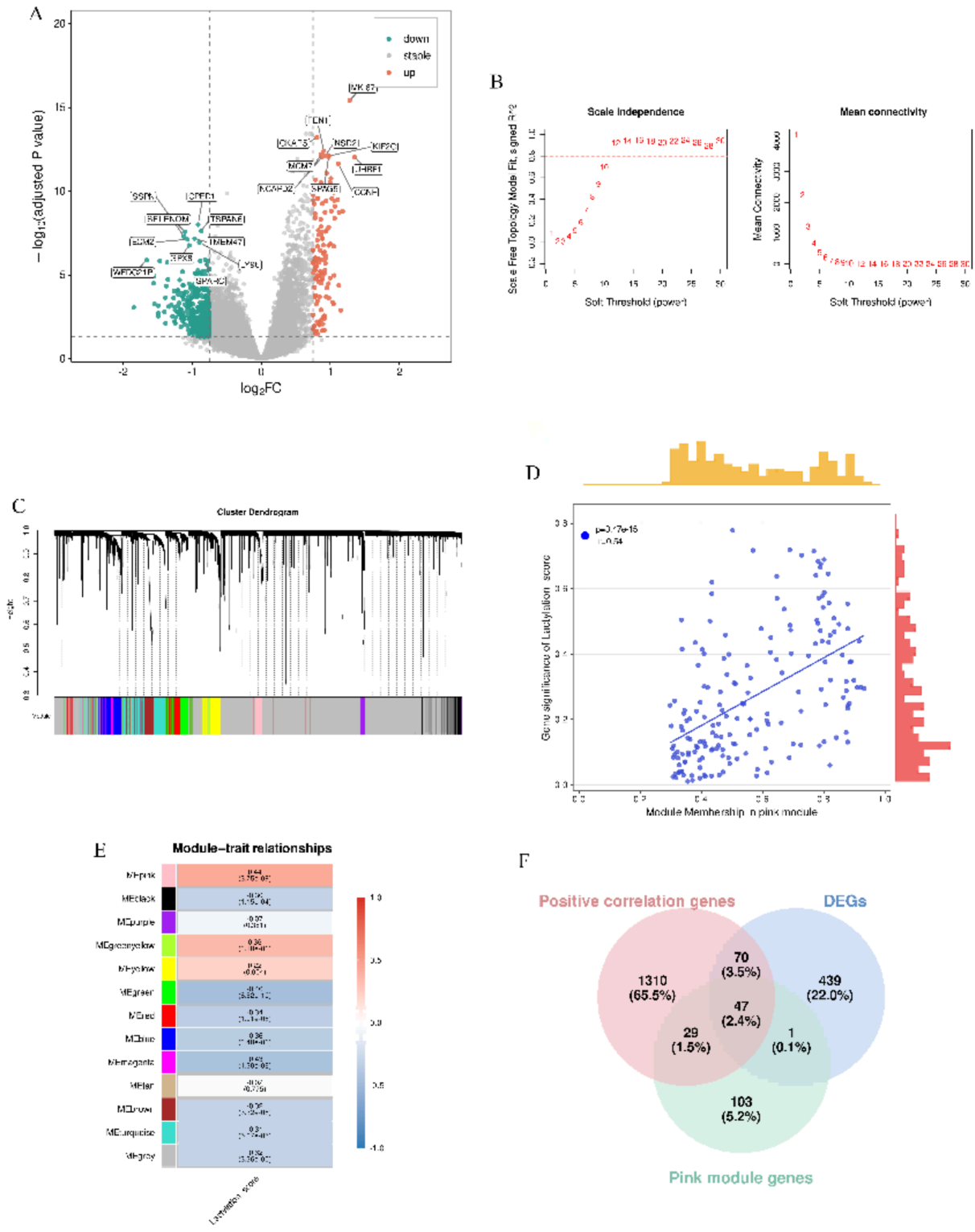


Figure 2

Differential expression analysis and WGCNA-based screening of lactylation-related candidate genes in PTCL

(A) Volcano plot of differentially expressed genes between the high- and low-lactylation-score groups. Orange indicates upregulated genes, green indicates downregulated genes, and grey indicates genes

without significant differential expression.

(B) Scale-free topology model fit index and mean connectivity across different soft-thresholding powers. β = 12 was selected to construct the co-expression network.

(C) WGCNA gene clustering dendrogram and co-expression modules identified by dynamic tree cutting. Different colours represent different gene modules.

(D) Scatter plot showing the correlation between module membership and gene significance for the lactylation score within the pink module. Marginal histograms show the corresponding distributions.

(E) Correlation heatmap showing the relationships between module eigengenes and the lactylation score. Correlation coefficients and P values are indicated.

(F) Intersection of genes positively correlated with the lactylation score, differentially expressed genes, and genes in the pink module, yielding 47 lactylation-related genes.

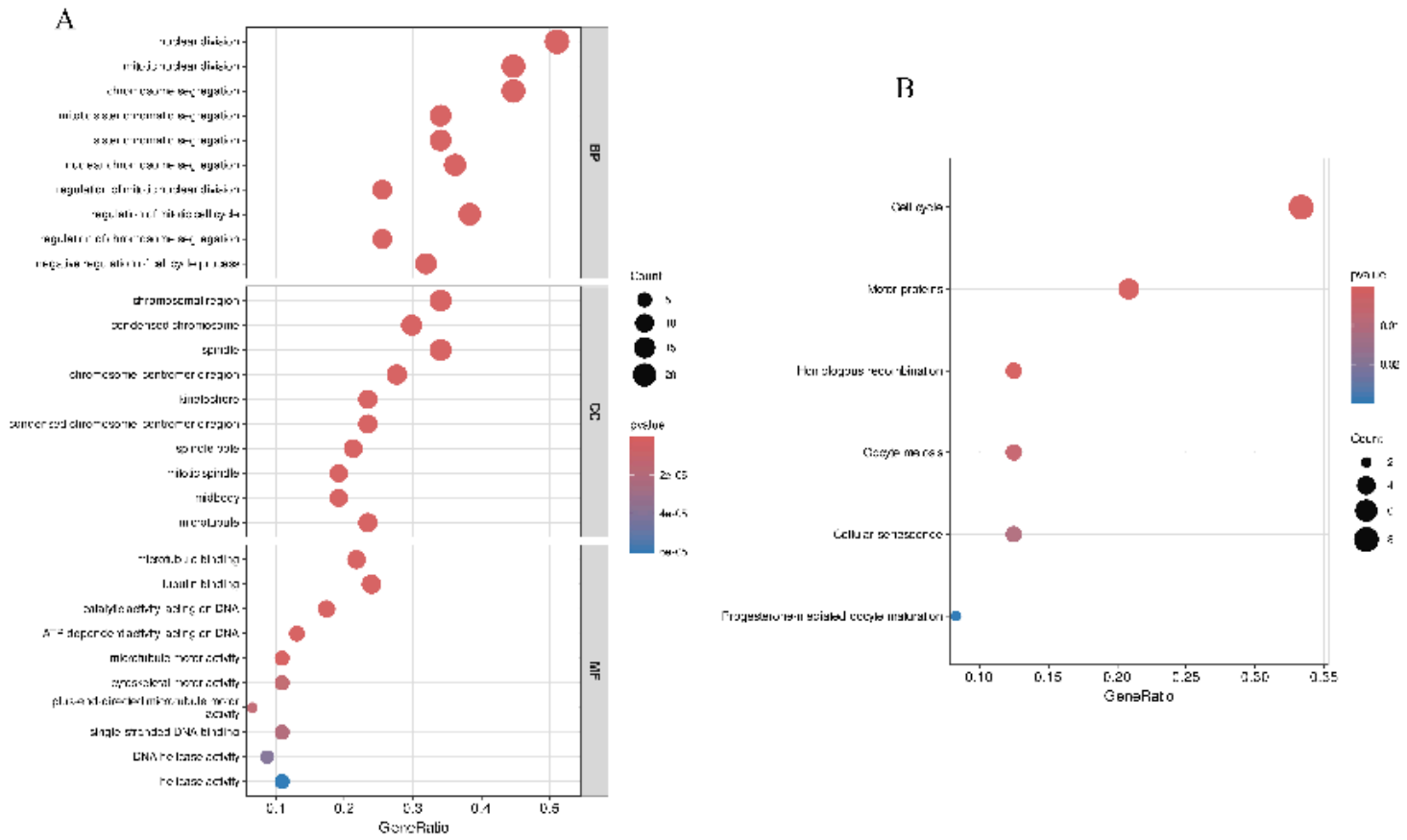


Figure 3

Functional enrichment analysis of lactylation-related genes

(A) Gene Ontology enrichment analysis of the 47 lactylation-related genes, including biological process, cellular component, and molecular function categories.

(B) Kyoto Encyclopedia of Genes and Genomes pathway enrichment analysis of the 47 lactylation-related genes.

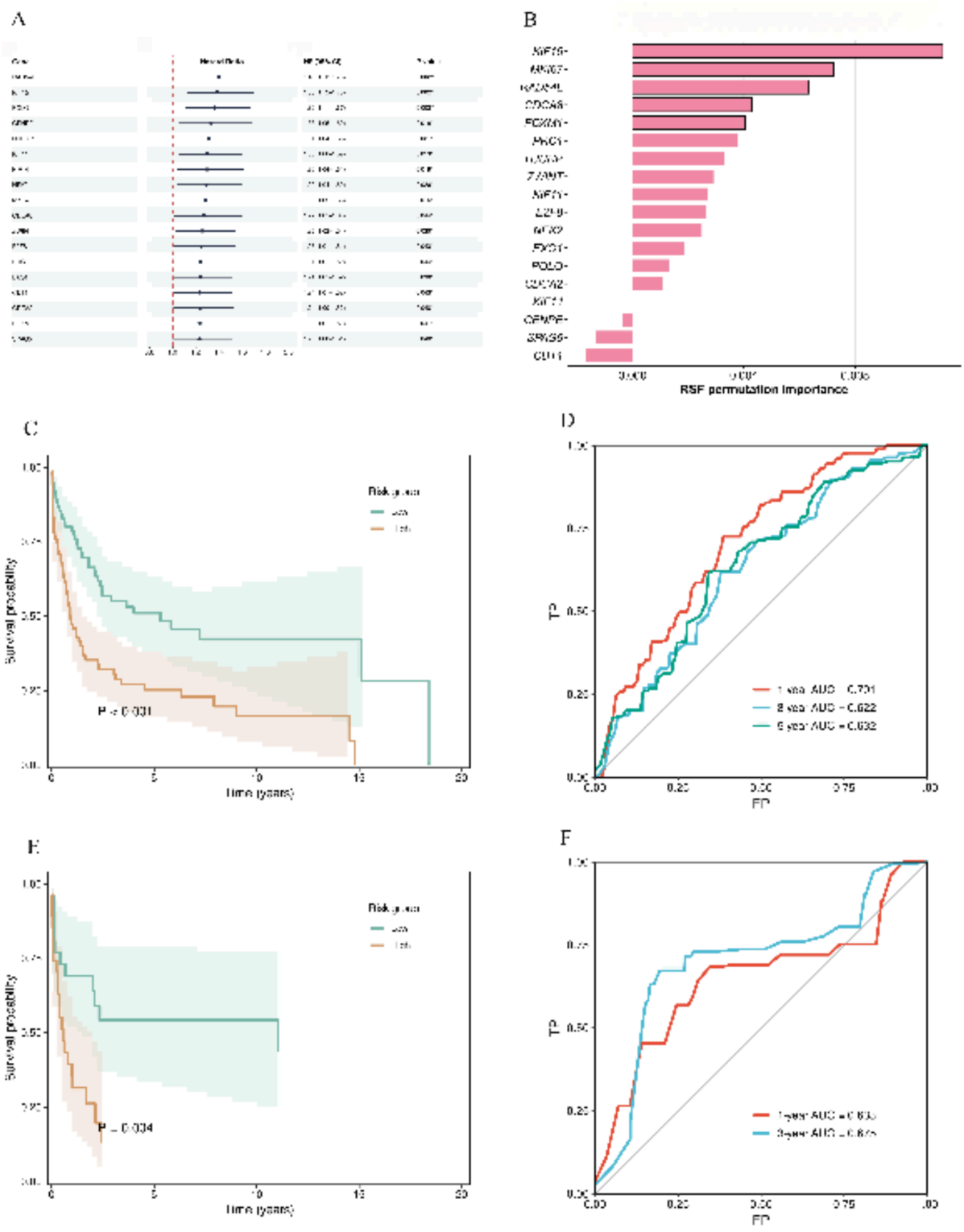


Figure 4

Construction and validation of the lactylation-related prognostic model

(A) Forest plot of univariate Cox regression analysis of the 47 lactylation-related genes.

(B) Random survival forest analysis assessing the importance of lactylation-related prognostic genes. The top five variables were selected for construction of the risk model.

(C) Kaplan–Meier survival analysis showed poorer overall survival (OS) in the high-risk group in the training cohort.

(D) Time-dependent receiver operating characteristic (ROC) curves of the lactylation-related risk model at 1, 3, and 5 years in the training cohort.

(E) Kaplan–Meier survival analysis showed poorer OS in the high-risk group in the validation cohort.

(F) Time-dependent ROC curves of the lactylation-related risk model at 1 and 3 years in the validation cohort.

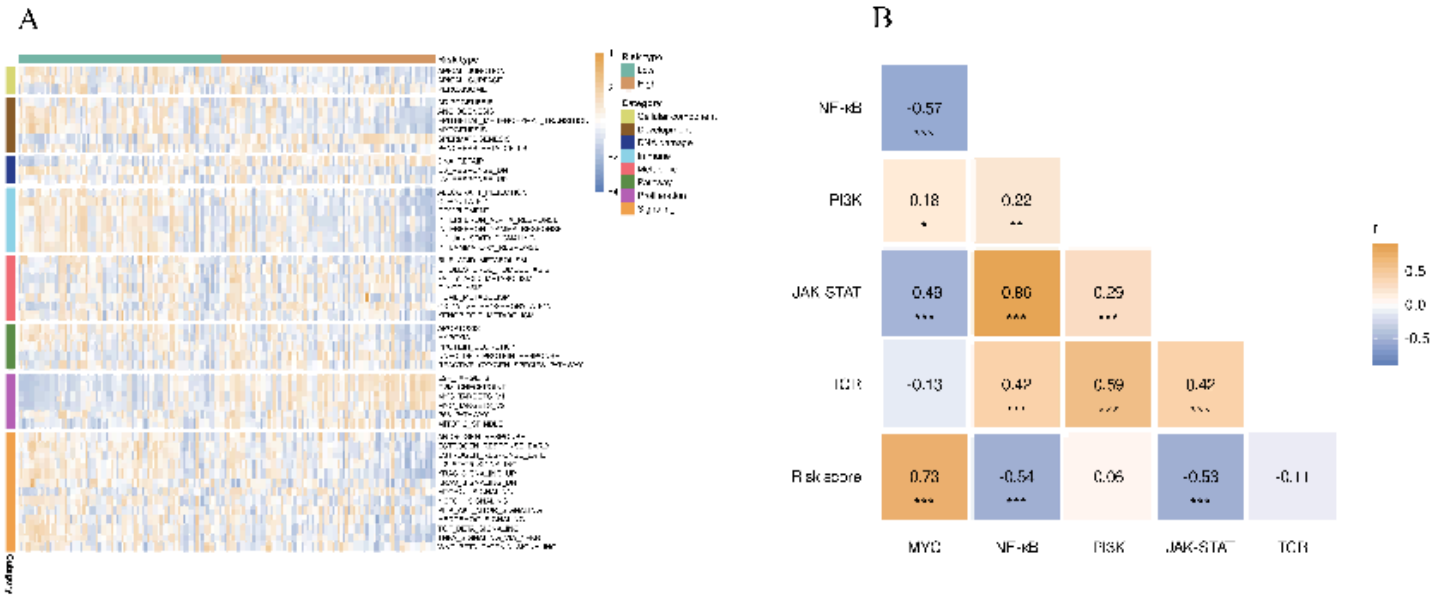


Figure 5

Differences in pathway activity between the high- and low-risk groups and correlations between the risk score and PTCL-related signalling pathways

(A) GSVA showing differences in Hallmark pathway activity between the high- and low-risk groups. Colour intensity represents pathway activity scores.

(B) Correlation matrix showing the relationships between the risk score and the activities of classical PTCL-related signalling pathways. Colour intensity represents correlation coefficients, and the numbers indicate the corresponding correlation coefficients.

*P < 0.05, **P < 0.01, and ***P < 0.001.

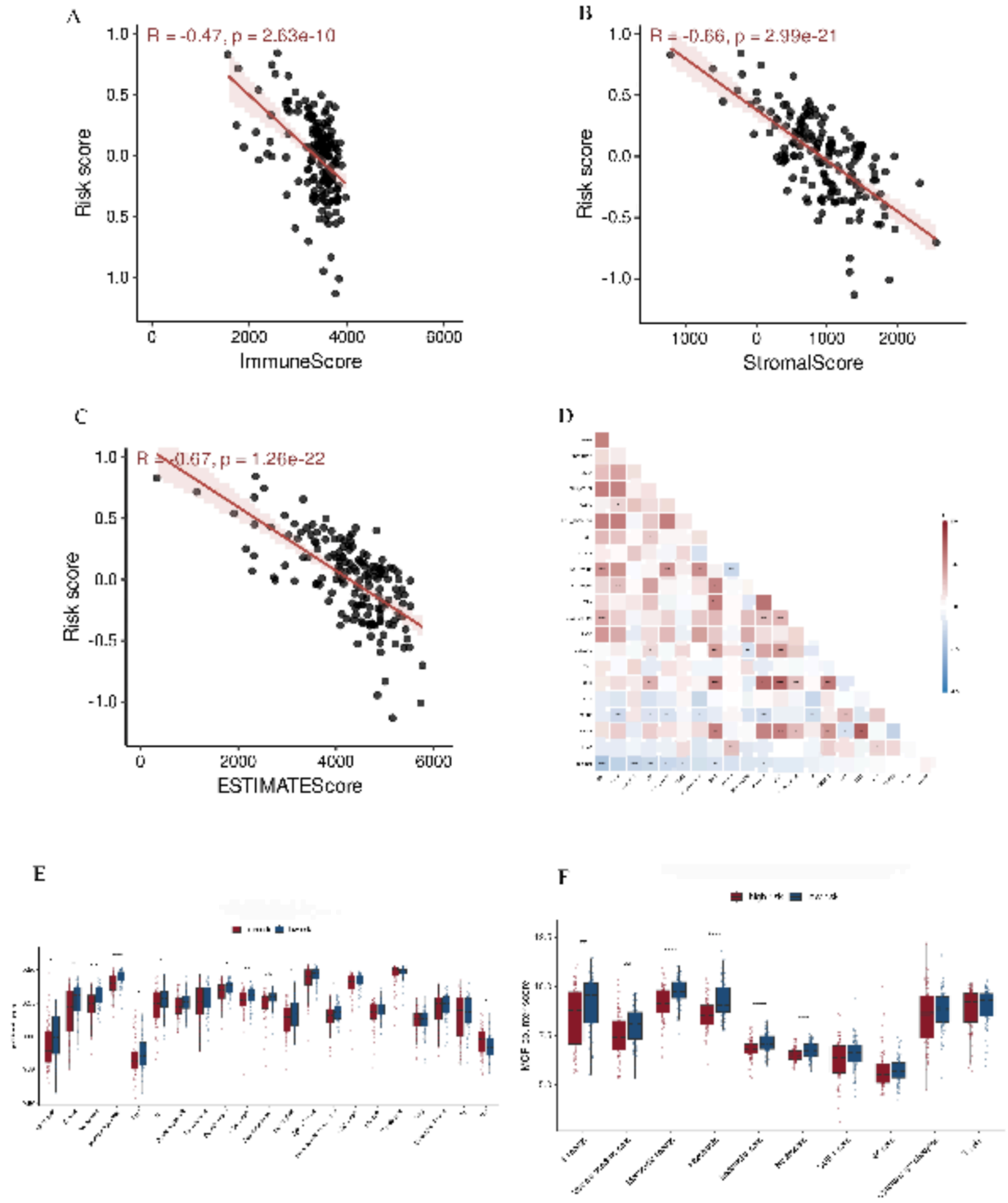


Figure 6

Association of the lactylation-related prognostic model with the tumour immune microenvironment in PTCL

(A–C) Correlation analyses of the risk score with the ImmuneScore, StromalScore, and ESTIMATEScore.

(D) Correlation matrix showing the relationship between the risk score and the expression of immune checkpoint-related genes. Colours represent correlation coefficients.

(E) ssGSEA showing differences in immune cell infiltration scores between the high- and low-risk groups.

(F) MCP-counter analysis showing differences in the abundance of tumour microenvironmental cell populations between the high- and low-risk groups.

*P < 0.05, **P < 0.01, ***P < 0.001, and ****P < 0.0001.

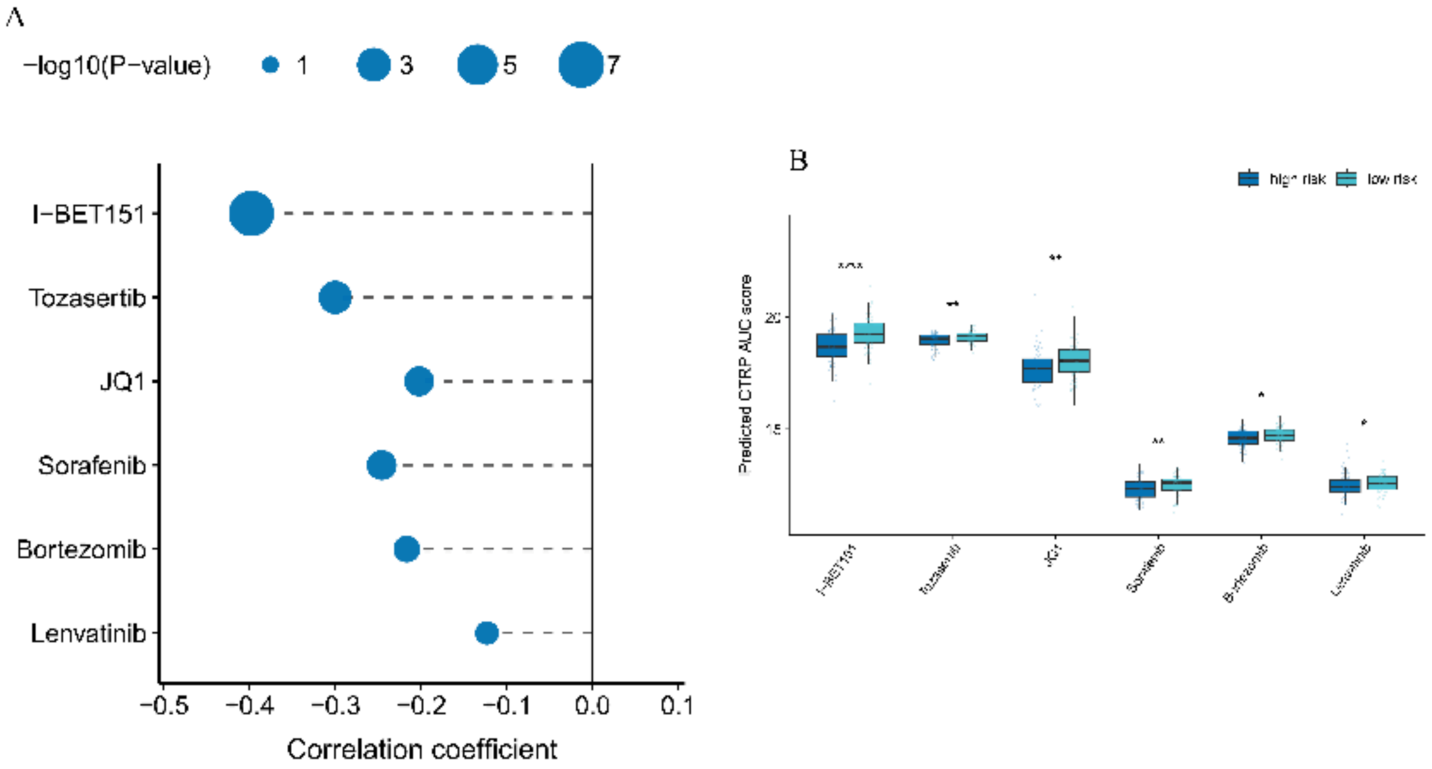


Figure 7

Drug sensitivity prediction based on the lactylation-related prognostic model

(A) Correlation analysis between the risk score and predicted AUC values for candidate drugs. The x-axis represents the correlation coefficient, and bubble size represents −log10 (P value).

(B) Differences in predicted AUC values for candidate drugs between the high- and low-risk groups. Lower predicted AUC values indicate greater predicted drug sensitivity.

*P < 0.05, **P < 0.01, ***P < 0.001, and ****P < 0.0001.

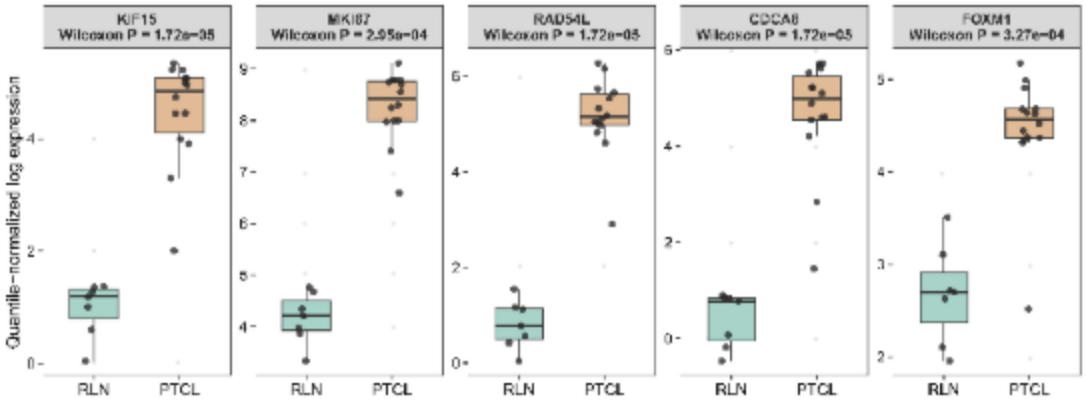


Figure 8

Differential expression of prognostic model genes between PTCL and reactive lymph node samples

Supplementary Files

This is a list of supplementary files associated with this preprint. Click to download.

- ESM1.xlsx
- ESM2.xlsx